Vol. **106** (2004) *ACTA PHYSICA POLONICA A* No. 1

Scattering of Lattice Waves in Planar Surface with Grafted Adatomic Chains

H. Aouchiche[a,*] and A. Kaddouri[b]

[a]Laboratoire de Mécanique, Structure et Énergétique
Université Mouloud Mammeri, Tizi-Ouzou, 15000 Algérie
[b]Equipe SIAM–UFR:MEC, Département de Physique
Faculté des Sciences Semlalia, Université Cadi Ayyad, Marrakech, Maroc

(Received November 6, 2003; revised version May 4, 2004)

In the present work the scattering properties of a monolayer atomic lattice with grafted adatomic chains are investigated. In the case of two grafted lines, separated by a fixed distance, the localized states induced by the defect are determined. The transmission spectra are also obtained for various distances between the two chains and for additional chains regularly spaced. On the one hand, some Fabry–Perot oscillations are observed; their number is directly related to the number of adatomic lines. On the other hand, Fano resonances due to interaction between the localized states and the continuum are obtained. When the mass value of the adatom decreases, it is shown that the resonances move towards high frequencies in agreement with the harmonic oscillator frequency. Another novelty in this work consists of the observation of zeros of transmission in the spectra.

PACS numbers: 61.46.+w, 63.50.+x, 63.20.Mt

1. Introduction

The phenomena occurring at the surfaces of solids are so complex that the researchers have addressed themselves to their studies for several decades with still a number of open questions. From fundamental research to the applied one, surface science progresses constantly and refines the knowledge of clean surfaces as well as of the ones covered with various adsorbates. It finds many applications particularly in the environmental protection technologies. It is also enhanced by

*corresponding author; e-mail: h_aouchiche@yahoo.fr

the practical interest in the modern technology field, e.g. catalysis, corrosion, metallurgy, and microelectronics. Several models [1, 2] were proposed to describe the ordered surface. The study of dynamical phenomena at disordered surfaces by completely *ab initio* techniques is still a difficult task. Various methods used are essentially based on Landauer principle [3], in which the studied sample is represented by a series of scattering centers introduced to the volume or to the surface of the perfect waveguide. Most of these works concern electronic transport [4–6]. However, the vibrational phenomena in disordered systems have not been studied with the attention they deserve. Because of the technology progress, the interest in the interference phenomena has been renewed in the two recent decades. We mention the matching method proposed by Feuchtwang [7] revised and improved by Szeftel and Khater [8]. Since then, it has not ceased to be applied to electronic phenomena [4–6] and waves scattering [9–15]. It is expected that the waves scattering would be more complicated there, because it involves a 3D vector field describing the components of displacements at each site, contrary to the electronic case, where the field is a scalar. In addition, the interactions between various eigenmodes of the perfect waveguide make the transmission and reflection spectra [14] more complicated.

During the past two decades, several theoretical and experimental studies treating perturbed surfaces have been formulated [10–17]. Berthod et al. [5] investigated the influence of a local defect on dc transport in mesoscopic quantum wires of finite width. They calculated the conductance [5] within the Landauer approach [3]. Fellay et al. [9] treated a planar quasi-one-dimensional waveguide composed of interconnected chains in harmonic approximation. They introduced local defects by changing the spring constants or the masses of the perfect waveguide. In both cases, they observed Fano resonances in the spectra. Khater et al. published the first paper [11] using the matching method applied to a linear chain. In their work the one-dimensional model is presented for surface phonon scattering channel by atomic inhomogeneities along a high symmetry direction in a solid surface. The linear chain model [11] yields characteristic resonances over the full Brillouin zone, for a monoatomic step and for an adatom. Additional resonances are found near the step edges for a symmetric double step. In addition, Virlouvet et al. [13] presented the dynamics for a model treating the monoatomic step as the interface between two coupled semi-infinite and single semi-infinite atomic layers. The step, considered as a structural defect, gives rise to several Rayleigh-like branches localized in the neighborhood of the perturbed region. The dispersion curves and Green functions are given and the spectral densities are presented for atomic sites that constitute the step region. In another paper, Virlouvet et al. [14] investigated the waves scattering at the step of the previous model [13]. Resonances due to a coupling between propagating continuum and localized states induced by the defect are observed. In addition, the influence of linear defect boundaries on the transmission and scattering of elastic waves

in quasi-two-dimensional waveguides is studied [15]. Then, the authors analyzed the dispersion curves, the attenuation factors and confirmed the presence of Fano resonances in the transmission spectra.

In the very recent years, the evolution of technology in atoms manipulation permits one to place individual atoms on a substrate using a scanning tunneling microscope. Based on the work of Eigler and Schweizer [18], who have constructed lines of Xe atoms on Ni substrate, we investigate a scattering of lattice waves in

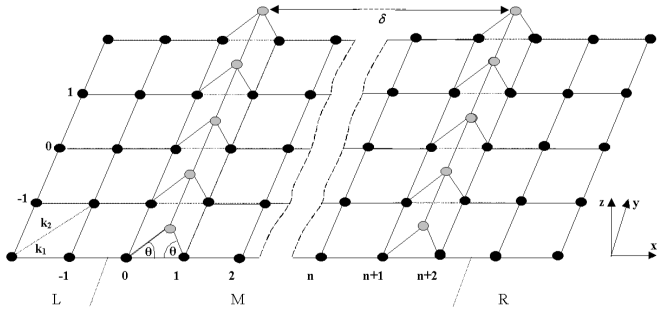

Fig. 1. Planar surface with grafted adatomic chains separated by a distance δ. M represents the defect region, L and R — two semi-infinite perfect waveguides.

planar surface with grafted adatomic chains (Fig. 1). The perfect waveguide properties have been already analyzed [19]. As a result, we show that the grafted chains give rise to some interesting scattering properties. We first describe briefly the analyzed atomic lattice and then, the principal stages of the matching method [9].

2. Calculation principle

The treated model (Fig. 1) is made of a monolayer atomic lattice surmounted by two atomic linear chains, which are separated by a distance $\delta = na$, where a is the parameter of the lattice and n is a positive integer. The two chains constituting the defect are laid out parallel to the y axis. All the masses forming the adatomic chains are identical. On the left and right of the perturbed area, denoted by M there, two semi-infinite perfect waveguides, L and R, extend. The considered interactions between atoms are those of an elastic spring with the force constants k_1 for the nearest and k_2 for the second nearest neighbors, respectively. To consider the modification of the bonding strength field in the perturbed area, we define a parameter λ indicating the ratio between the modified force constant of the adatoms and those of the perfect lattice located at equivalent sites.

2.1. Perfect waveguide

We present the propagating characteristics of a perfect waveguide, introducing the essential features of the formalism, which we will need later on. The

vibrational dynamics of the perfect waveguide is described by equations of Newton type defining the displacement amplitudes $u_\alpha(l,\omega^2)$ at a site l along the α direction at the vibrational frequency ω. The equation of motion of an atom is usually given [20], within the harmonic approximation framework, by the following expression:

$$\omega^2 m(l) u_\alpha(l,\omega^2) = -\sum_{l'\neq l}\sum_{\beta} k(l,l')\frac{r_\alpha r_\beta}{d^2}[u_\beta(l,\omega^2) - u_\beta(l',\omega^2)], \tag{1}$$

where α and β denote the space directions; $m(l)$ indicates the atom mass located at the site l, r_α is the component of the relative position vector between sites l and l', d — the distance separating them and $k(l,l')$ — the bonding strength constant between the two sites. The dynamical equations of various atoms of the perfect lattice are reduced to the linear system

$$[\Omega^2 I - D(\varphi_y, z, r_2)]|\boldsymbol{u}\rangle = |\boldsymbol{0}\rangle, \tag{2}$$

where $\Omega = (m\omega^2/k_1)^{1/2}$ is the normalized frequency without dimension, $r_2 = k_2/k_1$ the ratio of the force constants between the second and the first nearest neighbors, φ_y is the component of the incident wave vector along y direction and the parameter z is the phase factor $\exp(\mathrm{i}\boldsymbol{q}a)$, where $\boldsymbol{q}$ is the wave vector parallel to the surface. The symbol I represents the identity matrix and D — the perfect lattice dynamical matrix. The numerical solution of the system (2), for progressive waves, delimits the allowed bands and the forbidden ones. We determine the terms in z and $1/z$ contained in the dynamical matrix D according to the frequency Ω. Only the solutions, whose module of z is equal to one (phase factors) or lower than one (attenuation factors), are considered. Thus, by establishing the values of $|z| < 1$, the extent of the evanescent field is rigorously determined. It does not contribute to the energy transport but it is indispensable in the calculation of the localized states.

2.2. Perturbed waveguide

It is known that the perfect waveguide does not couple different vibrational eigenmodes [20], so it is possible to treat the scattering problem for each mode separately. Thus, we can generalize this without difficulties to an incident wave, which would be an unspecified combination of the waveguide eigenmodes. For an incident wave coming from the left (Fig. 1) in the eigenmode $\overline{v}$ (the bar indicates the entering mode), the displacement $\boldsymbol{V}_{\mathrm{in}}^{(i)}$ of the site i can be expressed as

$$\boldsymbol{V}_{\mathrm{in}}^{(i)} = (z_{\overline{v}})^i \boldsymbol{u}_{\overline{v}}, \tag{3}$$

where $\boldsymbol{z}_v$ are the phase factors or attenuation ones and $\boldsymbol{u}_v$ — the eigenvectors, i indicates the order of the line containing the occupied site along the x direction. The waves resulting from an elastic scattering produced by the defect are composed of reflected and transmitted waves, which generate vibrational field in the

two perfect half spaces L and R. These components are expressed, via the matching method [9], as a combination of the waveguide eigenmodes. The expression of the reflected wave is given by

$$\boldsymbol{u}_{\mathrm{r}}^{i} = \sum_{v} \xi_{v\overline{v}} [1/z_v]^i \boldsymbol{u}(1/z_v) \tag{4}$$

and the transmitted one by

$$\boldsymbol{u}_{\mathrm{t}}^{i} = \sum \eta_{v\overline{v}} [z_v]^i \boldsymbol{u}(z_v), \tag{5}$$

where $\xi_{v\overline{v}}$ and $\eta_{v\overline{v}}$ become, after normalization by the group velocities, the reflection and transmission coefficients, respectively.

To write the equations of motion for the irreducible atoms (those of the defect area), we use the matching method to relate the atomic displacement components of the defect to those of the perfect lattice by the border atoms $(-1, y, 0)$ and $(n+3, y, 0)$. This procedure is carried out by isolating the inhomogeneous terms describing the incident wave. The results obtained are gathered in a matrix R, known as a matching matrix, whose elements are determined by the previous relations (4) and (5). Finally, the linear system can be expressed as follows [9]:

$$\left[\widetilde{D}\left(\Omega, \varphi_y, r_2, \lambda, z\right)\right] [R]\boldsymbol{X} = -\left[\widetilde{D}\left(\Omega, \varphi_y, r_2, \lambda, z\right)\right] \boldsymbol{V}_{\mathrm{in}}, \tag{6}$$

where $\widetilde{D}(\Omega, \varphi_y, r_2, \lambda, z)$ represents the defect dynamical matrix and $\boldsymbol{X}$ is the vector containing all the unknown terms (displacement components, transmission, and reflection coefficients).

3. Results and discussion

In this section, the obtained results are presented for only the defect region. The perfect waveguide characteristics have already been studied [19]; the data, which are needed in this work, are those obtained in Ref. [19]. We begin the section with the case of two adatomic chains represented in Fig. 1. In the second one, we comment the obtained transmission spectra in the case of regularly spaced adatomic lines. To our knowledge, no experimental results are available at present to compare with.

3.1. Two separated adatomic chains

The present section is divided into three parts. The first one describes the localized states induced by the defect, the second one concerns the transmission coefficients for a fixed distance δ, and the third one treats the case where δ varies.

3.1.1. Localized states

We begin by fixing the distance δ to $3a$. To carry out the calculation, we choose the parameter $\lambda = 0.8$, the value already used in Refs. [11, 14]. In addition, the angle θ subtended by the adatom and its nearest neighbors is equal to $\pi/6$.

The obtained results for the defect already described in Fig. 1 are collected in Fig. 2. The circles represent the limits, which separate the allowed bands and the forbidden ones, as functions of the wave vector component φ_y. The propagating continuum contains two modes, transverse and longitudinal [19]. We notice the presence of a small window (around b) in the bulk, which is not allowed to the phonons propagating in the monolayer. It is shown [19] that its size is directly related to the r_2 value ($r_2 = k_2/k_1$). Then it becomes larger when r_2 increases.

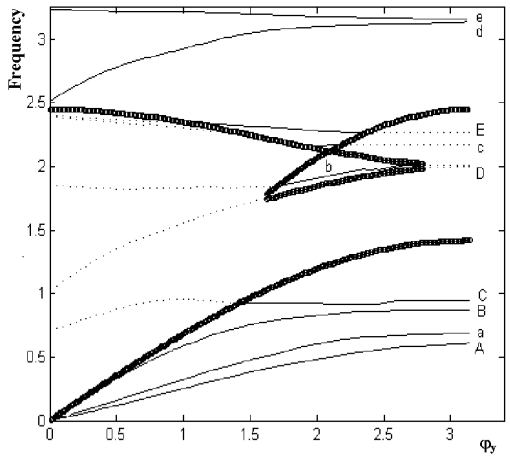

Fig. 2. Localized states of the structure of Fig. 1 with $\delta = 3a$. The curves noted in capital letters are associated to the heavy defect ($m' = 2m$), and those in small letters to the light one ($m' = 0.5m$). The circle curves indicate the limits of the propagation continuum. We notice a large window forbidden to the phonons.

In Fig. 2, the branches noted A, B, C, D, and E represent the localized states induced by the heavy defect ($m' = 2m$) and those noted a, b, c, d, and e are associated to the light one ($m' = 0.5m$). The state, indicated by a capital letter in the heavy mass case, is noted by the equivalent small letter in the light mass case. Several branches penetrate in the continuum (indicated by points in the bulk) and cross the propagating modes. This fact induces several interferences, as we shall see later. However, the branches A, a, d, and e do not interact with the continuum and therefore introduce no interference. The energy associated to the localized modes depends directly on the parameters λ and m'; then, while one of them varies, the branches shift and can entirely go into the continuum. For example in Fig. 2, we notice a shift towards the high frequencies when the mass of the defect decreases. The displacement of the different states is compatible with the classical harmonic oscillator energy. The different branches shift differently for the same frequency value and the different points of the same branch do not move regularly for each frequency. The phenomenon is so complicated that it is certainly difficult to find an analytical formula be-

tween the state shift value and the adatomic mass. In Ref. [14], one observes only two localized modes, contrary to this work, where we notice five. In our study, r_2 is taken equal to 0.5, consequently the window in the continuum is so large that it can contain localized states as shown in Fig. 2. In an isolated step [14], r_2 is equal to 0.05 then the window is so narrow that the localized states could not appear. In addition, the latter are calculated only outside the bulk. However, the general shape of these states is in qualitative agreement with the theoretical results of the isolated step [14] and vicinal surface [21].

3.1.2. Scattering for a fixed distance δ

The distance δ is always fixed at $3a$. The phonons scattered by the defect are analyzed relatively to an incident wave coming from the left (Fig. 1) with a unity amplitude and a null phase on the atomic site (–1,0,0). Figure 3 shows the obtained transmission coefficients in both transverse t_{11} and longitudinal t_{22} modes for heavy and light defect masses. The dotted curves represent the transmission coefficients in the case of one adatomic chain [19]. To avoid overloading of the figures, the reflection coefficients r_{11} and r_{22} are not reported. However, perfect complementarities between (t_{11}, r_{11}) and (t_{22}, r_{22}) are noted. During the interaction, the well-known physical conservation laws give rise to the conservation of the amplitudes such as $r_{11}+t_{11}=1$ ($r_{22}+t_{22}=1$). Moreover, along all this work, the equality is used as a control of the correctness of our results. The second significant remark lies in the oscillations presented by these different curves. The two defect chains, containing identical atoms and placed symmetrically relatively to the y axis, have the characteristics of Fabry–Perot resonator. Therefore, we must expect, in the spectra, Fabry–Perot (FP) oscillations due to interferences between the multiple scattered waves. Thus, the geometrical form of the defect explains the origin of the obtained oscillations. Moreover, in the case of only one adatomic chain [19], they are absent (dotted curves). For the light defect ($m'=0.5m$), these oscillations are always pronounced at middle and high frequencies, contrary to the heavy mass ($m'=2m$), where they appear clearly in the whole frequency range.

In the transverse mode and heavy defect, we observe a peak at $\Omega=0.63$ (Fig. 3c) overlapped with the FP oscillation structure. It is identified as Fano resonance due to the interaction at $\varphi_y=0$ between the localized state (branch C in Fig. 2) and the propagating continuum. In the light mass case (Fig. 3a), this resonance does not appear because the localized state moves to high frequencies and cross the Ox axis at $\Omega=2.38$ (Fig. 2), outside the frequency range of the transverse mode. This shift permits to assign the peak at $\Omega=2.38$ in Fig. 3b to Fano resonance (the interaction between branch c and the continuum), while the peak at $\Omega=1.8$ is attributed to the interaction between the continuum and the localized state noted b in Fig. 2. The two structures indicated by arrows in Fig. 3d are the results of the interaction between the bulk and the branches C and D (Fig. 2). Note that the branch C induces a resonance at $\Omega=0.63$ in both

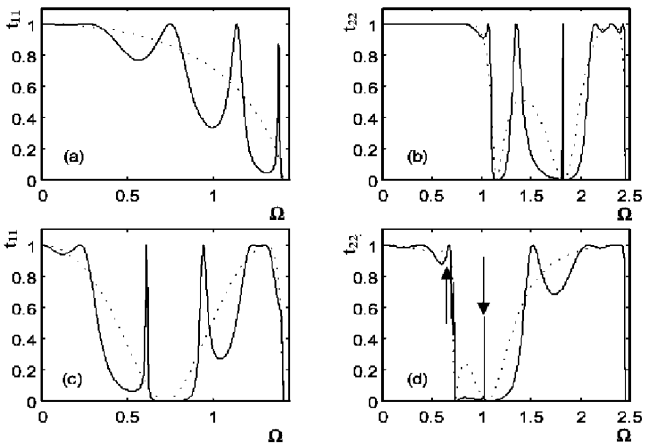

Fig. 3. Transmission coefficients in the transverse mode (t_{11}) and longitudinal one (t_{22}) as a function of the frequency for a distance $\delta = 3a$. In figures a and b: $m' = 0.5m$, in c and d: $m' = 2m$. Dotted curves represent the transmission coefficients in case of one adatomic chain (Ref. [19]).

transverse and longitudinal modes (Fig. 3c and d). This fact can be explained by the localized state mode, which certainly has components along Ox and Oy axes. We notice that the transmission coefficient does not necessarily reach a unit near the resonance, as it is usually the case. Such behavior is already observed in the case of an isolated step [14], where it is explained by a coupling between acoustic and optical propagating modes. The phenomenon has no analogue in the electronic waveguide [5]. In addition, according to their form, these resonances can be used to construct frequencies filter [22]. Finally, without counting the FP oscillations, the global shape of the various transmission curves is identical to those obtained for an isolated defect [19]. The same remark is also valid for the reflection coefficients.

In both transverse and longitudinal modes, the resonances shift towards the high frequency while one passes from heavy to light mass. This fact can be explained by the shift of the localized states, which move towards the high frequency when the mass decreases. A simple comparison with the harmonic oscillator frequency expression, $\omega = \sqrt{k/m}$, shows that the decreasing of the mass involves an increase in the frequency, consequently in the localized energy states. Thus, it is possible that the states will be located outside the bulk, when the mass becomes very small, and will not cross the propagating continuum. Consequently, the Fano resonances will disappear in the transmission spectra.

3.1.3. Transmission for variable distance δ

We introduce the transmission spectrum evolution according to the distance δ ($\delta = q_1 a$). In Fig. 4 the transmission spectra are shown as functions of the

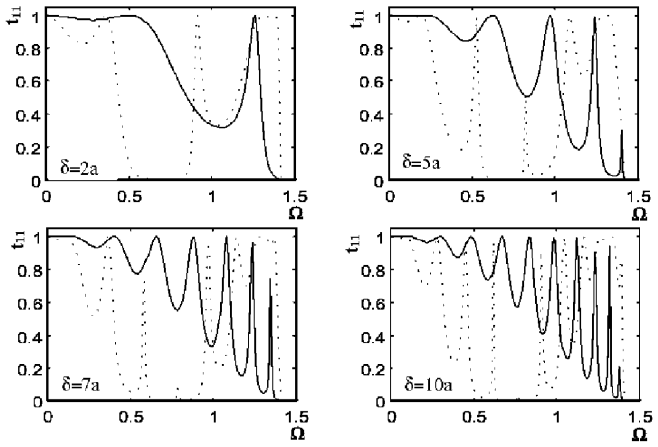

Fig. 4. Transmission coefficients in the transverse mode as a function of the normalized frequency for a defect composed of two atomic chains separated by a variable distance δ. Continuous curves are associated to the light mass ($m' = 0.1m$) and the dotted curves to the heavy one ($m' = 2m$).

normalized frequency Ω in the transverse mode for various distances δ. The dotted curves are associated to the heavy mass ($m' = 2m$) and the continuous ones to the light one. The light mass value is chosen $m' = 0.1m$ because the spectra present no Fano resonances and the FP oscillations appear clearly. Their number depends on the distance δ. First, consider the case of a light mass, the FP oscillations number increases with δ and dominates the entire spectrum. Their number is given by $s = q_1 - 1$. In the case of the heavy defect (dotted curves), we observe again FP oscillations which dominate the spectra, their number is always given by $s = q_1 - 1$. In this case, new fine structures, located at different frequencies and overlapped with the FP oscillations, are observed. They are assigned to Fano resonances. Note that the resonance peaks move slowly towards the weak frequencies when the distance δ increases.

In the case of longitudinal mode, the obtained results are reported in Fig. 5. For the light defect, we find an oscillatory behavior like in the transverse mode. As expected for the heavy defect, the difference between the two modes appears in the number of Fano resonances and in the FP oscillations, which are less symmetrical. Certainly, the increase in the number of resonances and their overlapping with the FP oscillations make these latter lose their symmetry. Moreover, as it is explained previously by the frequency expression of the harmonic oscillator, the increase in the mass value permits one to observe several localized states situated in the energy range of the bulk.

It is known that the resonating grafted chains introduce zeros of transmission in the electron transmission spectrum of an infinite backbone [23]. In the case of local defects on the dc transport in mesoscopic quantum wires of finite width [5],

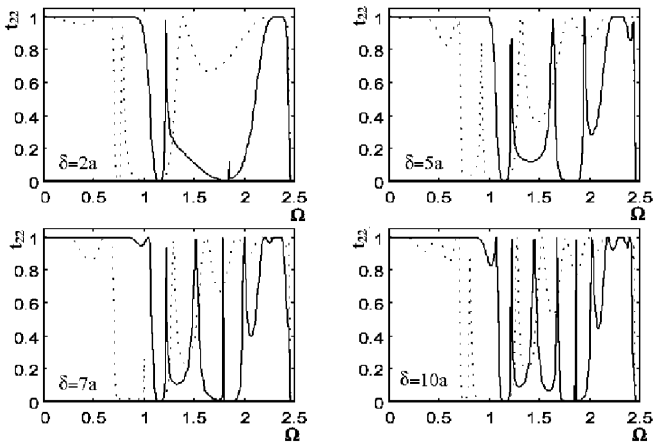

Fig. 5. Transmission coefficients in the longitudinal mode as a function of the normalized frequency for defect composed of two atomic chains separated by a variable distance δ. Continuous curves are associated to the light mass ($m' = 0.1m$) and the dashed curves to the heavy one ($m' = 2m$).

it was possible to find analytically the position of the zeros of transmission. In the present work, the polarisable waves are vectors, not scalars as in quantum wires, and each atomic site in the defect area (Fig. 1) has two or three degrees of freedom. The dimension of the system of linear equations (Eq. (6)) becomes very large, making the analytical expression of zeros of transmission impossible. In the case of the heavy defect, the results in Fig. 4 present frequency zones where the transmission is forbidden. For $\delta = 7a$ and $10a$ the zeros of transmission zone is divided in two intervals by a little peak. This zone remains constant when the number of defect chains increases. Note that in the case of a light defect, the zeros of transmission do not exist in the entire spectrum. For the longitudinal mode (Fig. 5) and in both cases (heavy and light defects), we observe two zones of zeros of transmission for $\delta = 2a$ and $5a$ and three zones for $\delta = 7a$ and $10a$.

3.2. Regularly spaced adatomic chain sequences

Kushwaha et al. [24] have investigated sequences of dangling side branches grafted on equidistant sites of a one-dimensional slender tube. Thus, we introduce the defect chains in the way to form sequences of regularly spaced lines. Our work is generalized to two dimensions. In Fig. 6 the obtained transmission spectra are presented in both vibrational modes for three adatomic sequences with light defect ($m' = 0.1m$) and heavy one ($m' = 2m$). To simplify the representation, the analyzed structures are shown in two dimensions (Ox, Oz) above each figure. As previously, we observe FP oscillations and Fano resonances. In the transverse mode, the transmission is strongly affected even at low frequencies contrary to the preceding cases, where it is total at the beginning. When the chain number

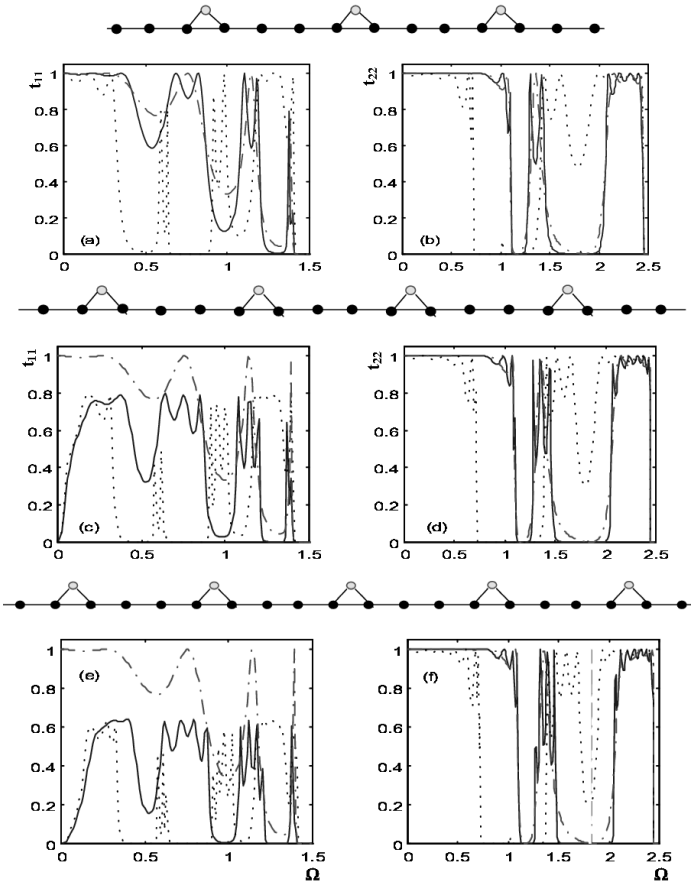

Fig. 6. Transmission coefficients as a function of the normalized frequency in transverse mode (a, c, and e) and longitudinal (b, d, and f) for defect sequences. The atomic structure scheme is given in two dimensions (Ox, Oz) above each figure. The continuous curves are associated to $m' = 0.1m$ and the dotted to $m' = 2m$. The dashed curve is associated to a sequence of two defects separated by $\delta = 3a$.

exceeds three, the transverse transmission coefficient t_{11} tends toward zero for Ω tending to zero. On the contrary, the coefficient t_{22} keeps the value of its intensity at the range beginning while oscillating slightly; the defect opposes a resistance to the passage of the transverse wave. When the defect is composed of five lines, the intensity decreases about 40% in all the propagation range of the transverse mode. While introducing seven chains, we notice an intensity reduction of 60% (not reported here). This kind of behavior seems rather strange, since, in general, the sound transmission at low frequency is not deteriorated by the local defects as it is shown by the precedent spectra. However, this phenomenon can be explained by considering that the waves interfere in a destructive way between each pair

of defect atoms. The cumulative effect between these different pairs makes that transmission intensity is reduced more and more. It is even probable to obtain a total reflection if the sequence is made up a high number of rows. Note that the intensity in the longitudinal mode is not affected in both heavy and light masses. The higher number of oscillations and resonances makes spectra not clear (Fig. 6e, f) so it is difficult to conclude on the effect of an increasing number of lines.

In the case of the longitudinal mode, the zeros of transmission are also observed for the two cases of adatomic masses, whereas for the transverse mode only the heavy defect presents forbidden transmissions. In addition, the FP oscillations lead to a separation in bands (for example in Fig. 6c: 0–0.5, 0.5–1, 1–1.3), which depend strongly on the atoms number located between adjacent adatomic lines and consequently on the distance separating them. The global shape of the curves is similar to that of the defect made of two adatomic chains separated by the same distance δ (dashed curves in Fig. 6). On each transmission band, one distinguishes small oscillations, which depend directly on the entire width of the defect area. If q_2 indicates the number of adatomic lines of the sequence, the structures appearing in each spectrum are effectively subdivided into $q_2 - 1$ substructures. This subdivision looks so that the number of substructures is equal to the number of intervals separating the particular lines.

4. Conclusion

In this work, we developed an approach permitting the treatment of the waves scattered by a structural defect. We directly solve the Newton dynamical equations by using wave functions represented by vectors. So, our work constitutes a support for the study of the interferences phenomena introducing polarised waves such as electromagnetic ones. In addition, we observe that the defect influences directly the perfect waveguide behavior by creating its proper energy states localized in the perturbed area. These states interact with the continuum. Thus, we show that some phenomena in particular Fano resonances, which had been observed in the case of electronic transport [5], occur also for scattering waves. Moreover, we show that resonance peaks move toward high energies for light masses in agreement with the isolated harmonic oscillator frequency. Thereby, when the adatomic mass value becomes very light, all resonances or some of them disappear from the bulk. We conclude that this procedure can be used as a method allowing the evaluation of the mass of the defect by the frequency limit value; then one can characterize the defect nature of the structure.

The waveguides have the geometrical characteristics of Fabry–Perot resonators. Thus, these oscillations, which are well known in optic, are also observed in the case of phonons. We show that their number depends on the adatomic chains number. We note that the presence of the defect modifies considerably the dynamical and thermal properties of the lattice by introducing Fano resonances,

Fabry–Perot oscillations, and zeros of transmission. In addition, it was observed that the transmission spectra intensity decreases gradually when the chains number increases. Therefore, the intensity of the spectra can be used to identify the defect size.

References

[1] R.E. Allen, G.P. Alledredge, F.W. Wette, *Phys. Rev. B* **4**, 1648 (1971).

[2] M.C. Desjonquéres, D. Spanjaard, *Concept in Surface Physics*, 2nd ed., Springer, Berlin 1996 and references inside.

[3] R. Landauer, *J. Phys., Condens. Matter* **1**, 8099 (1989).

[4] F. Gagel, K. Maschke, *Phys. Rev. B* **52**, 2013 (1995).

[5] C. Berthod, F. Gagel, K. Maschke, *Phys. Rev. B* **50**, 18299 (1994).

[6] E. Tekman, P.F. Bagwell, *Phys. Rev. B* **48**, 2553 (1993).

[7] T.E. Feuchtwang, *Phys. Rev.* **155**, 715 (1967).

[8] J. Szeftel, A. Khater, *J. Phys. C, Solid State Phys.* **20**, 4725 (1987).

[9] A. Fellay, F. Gagel, K. Maschke, A. Virlouvet, A. Khater, *Phys. Rev. B* **55**, 1707 (1997).

[10] J. Szeftel, A. Khater, F. Mila, S. d'Addato, N. Auby, *J. Phys. C, Solid State Phys.* **21**, 2113 (1988).

[11] A. Khater, N. Auby, D. Kechrakos, *J. Phys., Condens. Matter* **4**, 3743 (1992).

[12] Y. Pennec, A. Khater, *Surf. Sci. Lett. L* **82**, 348 (1996).

[13] A. Virlouvet, H. Grimech, A. Khater, Y. Pennec, K. Maschke, *J. Phys., Condens. Matter* **8**, 7589 (1996).

[14] A. Virlouvet, A. Khater, H. Aouchiche, O. Rafil, K. Maschke, *Phys. Rev. B* **59**, 4933 (1999).

[15] M. Belhadi, O. Rafil, R. Tigrine, A. Khater, J. Hardy, A. Virlouvet, K. Maschke, *Euro. Phys. J. B* **15**, 435 (2000).

[16] A. Lock, J.P. Toennies, G. Witte, *J. Electron Spectrosc. Relat. Phenom.* **54/55**, 309 (1990).

[17] G. Witte, J. Braun, A. Lock, J.P. Toennies, *Phys. Rev. B* **52**, 2165 (1995).

[18] D.M. Eigler, E.K. Schweizer, *Nature* **344**, 524 (1990).

[19] H. Aouchiche, M.S. Rabia, to appear in *Sciences & Technologie*.

[20] A.A. Maradudin, E.W. Montroll, G.H. Weiss, I.P. Ipatova, *Theory of Lattice Dynamic in the Harmonic Approximation*, Academic Press, London 1971.

[21] E.J. Mele, M.V. Pykhtin, *Phys. Rev. Lett.* **75**, 3878 (1995).

[22] M. Guglielmi, F. Montauti, L. Pellgrini, P. Acioni, *IEEE Trans Microwave Theory Technol.* **43**, 1911 (1995).

[23] W. Porod, Zhi-an Shao, C.S. Lent, *Appl. Phys. Lett.* **61**, 1350 (1992).

[24] M.S. Kushwaha, A. Akjouj, B. Djafari-Rouhani, L. Dobrzynski, J.O. Vasseur, *Solid State Commun.* **106**, 659 (1998).